Article type: Full paper

Study of the plasma-liquid interaction for an argon non-thermal microwave plasma jet from the analysis of benzene degradation

Enrique Casado, Maria C. Garcia, Dorota A. Krawczyk, Francisco-José Romero-Salguero, Antonio Rodero*

E. Casado
Department of Physics, University of Córdoba, Campus de Rabanales, Albert Einstein Building, Ctra. Nnal. IV, km 396, 14071, Córdoba, Spain
E-mail: casadoromeroe@gmail.com

Prof. M. C. García
Department of Applied Physics, University of Córdoba, Campus de Rabanales, Albert Einstein Building, Ctra. Nnal. IV, km 396, 14071, Córdoba, Spain
E-mail: fa1gamam@uco.es

Assoc. Prof. D. A. Krawczyk
Bialystok University of Technology, Wiejska 45 E, 15-351 Bialystok, Poland
E-Mail: dkrawcz@interia.pl

Prof. F.J. Romero-Salguero
Department of Organic Chemistry, Faculty of Sciences, University of Córdoba, Campus de Rabanales, Marie Curie Building, Ctra. Nnal. IV, km 396, 14071, Córdoba, Spain
E-mail: qo2rosaf@uco.es

Assoc. Prof. A. Rodero
Department of Physics, University of Córdoba, Campus de Rabanales, Albert Einstein Building, Ctra. Nnal. IV, km 396, 14071, Córdoba, Spain
E-mail: fa1rosea@uco.es

The interaction of an argon microwave plasma jet with a benzene layer on water has been studied under different conditions (power, gas flow, plasma-sample distance, and treatment time). Main products formed upon treatment are phenol, catechol, and nitrobenzene, showing this jet is source of radicals ·OH and $\cdot NO_2$ inducing benzene oxidation and nitration. Argon excited species in the plasma have been proven to play an outstanding role in degradation processes, which is mostly happening at the gas phase. Results are compared to those from direct interaction of the plasma jet with water. For this purpose, aqueous solutions of CCA are

treated, and the hydroxylation of this compound is studied. The effect of the benzene layer preventing water evaporation is demonstrated.

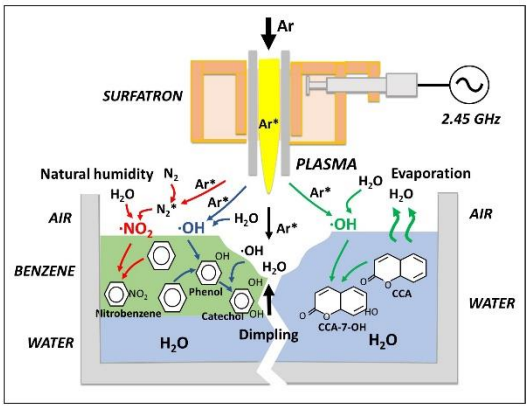

Keywords: *microwave discharge; oxidation; plasma jet; plasma treatment; plasma-liquid interaction; optical emission spectroscopy*

1 Introduction

In the last years, the study of the plasma-liquid interactions has gained high attention due to its relevance in a wide variety of applications including environmental remediation, material processing, nanoparticle synthesis, analytical chemistry, plasma medicine, food, and agriculture, among others.[1,2]

Non-thermal atmospheric pressure plasma jets (APPJs) have been investigated for this purpose, as they have attractive advantages including low power consumption and their ability to achieve enhanced gas-phase chemistry at relatively low gas temperatures. Here, the plasma-liquid interaction takes place in a plasma-over-liquid configuration.[1] Plasma jets can generate reactive species and flush them to a separate region for processing applications. This spatial separation provides a considerable flexibility in jet design in order to achieve good control in both plasma dynamics and interaction with liquid. Under this remote exposure, the effect of charged particles on the sample under treatment is weak as most of these species recombine before reaching it.

APPJs are being successfully utilized in the context of plasma medicine.[3-8] Treating human tissue to promote the healing of wounds, induce apoptosis in cancer cells, and kill bacteria are some of their most investigated applications.[9-14] Some of the reactive oxygen and nitrogen species (RONS) generated through the plasma jet action, such as O_3, the radicals ·OH, ·NO, $\cdot NO_2$, hydrogen peroxide (H_2O_2), excited singlet O_2 and peroxynitrous acid (ONOOH) have a direct impact on cells. These species compromise the integrity of the cell membrane and induce strong oxidative and nitrosative effects inside cells and many other mechanisms that are not well known yet, which makes them be the subject of ongoing research. Although RONS are not the only plasma components with influence on biological systems (charged particles, electric fields, UV radiation), they play an outstanding role in the whole plasma biological action.[15]

APPJs are also used for water remediation.[1,2,16,17] The plasma-liquid interaction results in the very same consumable used in advanced oxidation,[18,19] driving several physical and chemical advanced oxidation processes (AOPs) in water. Different plasma jets have been proposed as advanced oxidative technologies.[16,20]

In this work, the interaction of a non-thermal microwave argon plasma jet with liquid has been investigated through the study of the degradation of benzene. In a complementary way and shading light on the plasma-liquid interaction, the formation of OH species in water with the assistance of this jet was also analyzed. A *surfatron* was used as a microwave coupling device providing plasmas not spatially bound or confined by electrodes, so particularly useful for biological and environmental applications[21].

Nowadays, water contamination by organic pollutants (volatile organic compounds, pharmaceutical, dyes…) is dramatically growing, being an issue of serious concern that is attracting increasing attention worldwide. In this context, the improvement in the current technology for water purification arises as an urgent need. Benzene is an aromatic hydrocarbon, liquid at normal conditions of pressure and temperature. Colorless and highly flammable,

benzene is widely used in petrochemical, textile, pharmaceutical, among other industries. Thus, benzene is used to make other chemicals such as cyclohexane (for nylon and synthetic fibers), styrene (for plastics), and cumene (for various resins). It is utilized in the manufacturing of some types of rubbers, drugs, detergents, lubricants, dyes, and pesticides.[22] Benzene is also utilized as an additive in petrol to increase the octane rating. But benzene is not only formed from human activities but also natural processes including emissions from volcanoes and forest fires. It is also present in crude oil and cigarette smoke. Both the International Agency for Cancer Research and the United States Environmental Protection Agency have determined that benzene is carcinogenic and hematotoxic to humans.

In industrial wastewaters, the concentration of benzene could reach high values.[23] Besides that, new ways of water contamination by benzene are continuously being discovered. Thus, after the wildfire season in the western US in 2018, persistent contamination by benzene was detected in the water infrastructure in a Santa Rosa neighborhood.[24] Benzene was measured at levels as high as 500 ppb (California's limit is 1 ppb for drinking water) and the city embarked on a program of testing, research, and consultation with water scientists and engineers. It was finally reported the likely contamination process began when the exceptional intensity of fire created extreme heat that melted the plastic water pipes on burned properties as well as other plastic components in the water system. It was also realized benzene had absorbed into the pores of the plastic pipes and was gradually leaching out.

Two common treatment technologies reported to be effective for the reduction of benzene in water are adsorption and air stripping.[25] Adsorption is a physical method considered to be an efficient technology for removing contaminants from water. Granular activated carbon is widely used with this purpose, although fiberglass-supported activated carbon filters and synthetic carbonaceous resins have shown better removal efficiency than it. Adsorption methods do not actually treat benzene but simply shift it from the aqueous phase to the solid

phase, and benzene remains unaltered. Air stripping is another physical process implying the transfer of the compounds from water into the air, generally accomplished by injection of water into the air via spray systems.

Advanced oxidation processes have also been reported to be effective for the reduction of benzene in water, and more generally, for degrading recalcitrant materials and toxic contaminants.[26] AOPs refer to chemical processes and precursors that have high reduction potentials and either produce OH or directly attack organic molecules (ozone, atomic oxygen, excited nitrogen, ultrasound, UV light, and peroxide).[20] They are approaches allowing *in situ* decomposition of organic compounds in water through the conversion of the compound to carbon dioxide, water, and inorganic intermediates. The use of plasma technology to induce AOPs for water treatment purposes has notably grown in the last years.[27-31] Of particular interest are non-thermal plasmas at atmospheric pressure, which have been proven to be an efficient decontamination technology, having attractive advantages including low power consumption and their ability to achieve enhanced gas-phase chemistry at relatively low gas temperature. The potential of these plasmas to inactivate bacteria on surfaces[12-14] or destroy proteins[32] has already been proved. They have also been used for wastewater treatment,[18,20,33-35] both interacting directly plasma with water or remotely from some distance, showing efficient results.

The present work looks into the formation of hydroxyl radicals (·OH) and nitrate radicals ($\cdot NO_2$) by the abovementioned argon microwave plasma jet operating in front of a sample of benzene, through the study of reactions taking place between benzene and these radicals. Benzene was placed on a sheet of water, in order to increase the amount of ·OH radicals under certain experimental conditions. Products from these reactions were identified and quantified using Gas Chromatography-Mass Spectrometry (GC-MS) analysis under different plasma conditions, namely, microwave power, argon flow rate, time of treatment and plasma-liquid

distance. In this way, the formation of new products and their dependency on the ·OH radical production rate (measured by using fluorimetric techniques) was studied. For a better understanding of mechanisms leading to pollutant degradation, a plasma characterization (gas temperature and electron density) was done in all cases, using Optical Emission Spectroscopy (OES) techniques.

2 Experimental Section

2.1 Plasma reactor

An argon plasma jet was generated using a *surfatron* microwave power coupling device.[36] Surfatron coupled the energy coming from a microwave (2.45 GHz magnetron head) generator to the support gas (argon with a purity > 99.995%) within a T-shaped quartz reactor tube of 1.5 and 4 mm of inner and outer diameters, respectively, with one of its ends open to the air (see **Figure 1**). Although it was originally designed to generate cylindrical plasma columns inside straight dielectric tubes (TM_{00} surface wave mode), this particular tube configuration forced the plasma column to go down through its vertical part, making it easier to control the plasma-liquid distance.

This device has shown to be efficient in the degradation of methylene blue as water pollutant in a previous work[21], where argon excited states demosntrated to play an outstanding role in the oxidation of the pollutant. On the other hand, in this system, the interation plasma-liquid takes place at the post-discharge region, kinekics is expected mainly controlled by neutral species.[37UV radiation and electrons from plasma have a negligible effect on the sample.] On the other hand, experiments using a quartz glass only allowing the action of UV radiation on the samples (as it precluded the rest of species to reach the liquid), have shown the negligible effect of this radiation.

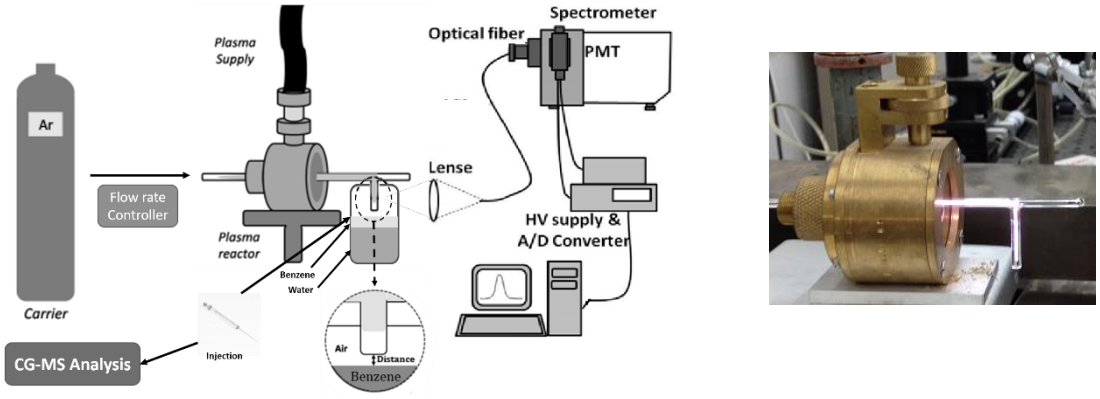

Figure 1. Experimental Setup

2.2 Liquid samples

Each experiment was performed three times under identical experimental conditions. In each case, fresh liquid samples were placed in cylinder-shaped glass containers (2 cm outer diameter, 1.6 cm inner diameter and 4 cm high). For the study of the oxidation of benzene, 1.5 ml of benzene (PanReac Applichem, purity > 99%) and 4 ml of mili-Q water were utilized. Benzene stayed on the top because of its nonpolar molecules and lower density. Phenol, catechol, and nitrobenzene (Alfa Aesar, purity > 99%) were used to calibrate the concentration of the resulting products.

A solution 0.003 M of 3-coumarin carboxylic acid (Aldrich, purity > 99%) in 4 ml of mili-Q water was used in experiments aiming at studying OH determination in aqueous solutions. Also, 7-hydroxycoumarin carboxylic acid (Aldrich, purity > 99%) was utilized for calibration of concentrations of this compound.

Preparation and later treatment of the samples were performed in a chemical fume hood.

2.3. Analysis methods

In this work, the liquid sample suffered a remote plasma exposure and plasma-liquid sample distance was changed from 0.5 to 4.5 cm (measured from the end of the plasma to the liquid

surface). Microwave power was set at different levels ranging from 30 to 90 W, and the argon flow rate (adjusted using a calibrated mass flow controller) was varied between 0.5 and 2 L/min. Unless for the case of P = 30 W, plasma went out of the vertical tube, whose length was constant (3 cm). Another parameter explored in this work was the treatment time, which was changed from 0.5 to 2 min. As shown in additional experiments, thermal degradation of the organic pollutant was negligible under the experimental conditions explored in this work.

Upon plasma treatme, benzene layer content was analyzed using a Gas Chromatograph-Mass Spectrometer (Thermo Finnigan, Thermo-Quest Trace GC/MS-Trace DSQ). Evaporation occurring in the sample during the treatment, due to the high volatility of benzene, was considered in terms of changes in concentration. For this purpose, samples were weighed before and after treatment in order to quantify the mass of benzene evaporated in each case.

The concentration of ·OH radicals in aqueous solutions treated with this jet was measured from the fluorescence method proposed by Newton and Milligan[37] based on the use of 3-coumarin carboxylic acid (CCA) as a chemical probe. This compound reacts with ·OH radicals by addition to the aromatic ring, being 7-hydroxycoumarin carboxylic acid (CCA-7-OH, which is fluorescent) one of the resulting products. Thus, the method consists of treating aqueous solutions 0.003 M of CCA dissolved and measures the amount of CCA-7-OH produced by fluorescence (spectrofluorometer PTI, Quanta Master 40 UC/VIS Steady State). Considering that the yield of the reaction of CCA with ·OH radicals is 4.7%, the concentration of ·OH radicals can be estimated.[37,38]

2.4. Plasma characterization

The gas temperature (T_g), the relative density of argon excited atoms in the state *4p* (n_{Ar4p}), and the electron density (n_e) at the edge part of the plasma tube were measured using OES techniques. **Figure 1** also shows a schematic of the material for OES measurements. The emission from the plasma was analyzed by using a 1 m focal length Czerny-Turner type

spectrometer, equipped with a 1200 grooves/mm holographic grating and a photomultiplier (spectral output interval of 300–900 mm) as a detector. The light emitted at the final position of the plasma (closest to the liquid) was side-on collected and focussed at 1:1 onto an optical fiber using an achromatic lens.

The relative population of argon excited atoms in the state *4p* (n_{Ar4p}) was measured from the intensity of the line Ar I 840.82 nm.[21] Under the experimental conditions of this work, *4p* states are highly populated and are moreover contributing to the formation of long-lived argon metastable states in the afterglow.[39-41] On the other hand, the collisional broadening of this line was utilized to determine the gas temperature following the method proposed by Rodero and García. [42] Thus, the profile of the recorded line was approximated to a Voigt shaped profile with a full width at half-maximum (FWHM), W_V, given by

$$W_V = \frac{W_C}{2} + \sqrt{\left(\frac{W_C}{2}\right)^2 + W_I^2} \qquad (1)$$

where W_C is the FWHM of the Lorentzian profile due to the *collisional broadening* (encompassing van der Waals, resonance and Stark broadenings), and W_I is the FWHM of the Gaussian profile due to the *instrumental broadening*. Under the experimental conditions of this work, both Stark and Doppler contributions to the whole broadening for the line Ar I 840.82 nm can be neglected (see reference [42] for more details).

The collisional broadening has two main contributions, van der Waals and resonance broadenings, and can be written as

$$W_C(T_g) \approx W_W(T_g) + W_R(T_g) = \frac{C_W}{T_g^{0.7}} + \frac{C_R}{T_g} \qquad (2)$$

being C_W and C_R constant values dependent on the line (C_W = 2.011, C_R = 67.519 Ar I 840.82 nm).

From equation (1) W_C can be obtained and expressed as

$$W_C = W_V - \frac{W_I^2}{W_V} \quad (3)$$

Therefore, by measuring W_V and knowing the value of the instrumental broadening, W_C can be derived from Eq. (3). Finally, the gas temperature can be determined using Eq. (2).

On the other hand, the electron density (n_e) was measured from the Stark broadening of the line H_β following a similar procedure. Under the experimental conditions of this work, the main collisional broadening for this line is due to the Stark effect. Its resonance broadening is negligible (as argon is the main gas), but the van der Waals one needs to be considered.[43] In this case, the mathematical expressions used in calculations were:[43-45]

$$W_C(T_g) \approx W_S(n_e) + W_W(T_g) \quad (4)$$

$$W_S(n_e) = 4.8\left(\frac{n_e}{10^{23} m^{-3}}\right)^{0.68116} \quad (5)$$

$$W_W(T_g) = \frac{4.10}{T_g^{0.7}} \quad (6)$$

The values of FWHM of the instrumental function for the wavelengths 486.32 and 840.86 nm, corresponding to the lines used in this work H_β and Ar I, using 77 µm width slits, were 0.06326 and 0.05884, respectively.

3 Results and Discussion

3.1. Interaction plasma-benzene: degradation of benzene

Products resulting from the interaction plasma-benzene were detected and quantified using CG-MS analysis. Different peaks identifying these products (whose areas are related to their concentrations) were observed in the chromatograms (see **Figure 2**). In this work, attention was focused on the three main products resulting from the degradation of benzene, namely, phenol, nitrobenzene, and catechol (benzene-1,2-diol), whose peaks appeared at 3.31 min, 4.56 min and

5.76 min retention times, respectively. Some other peaks were also detected, although they have not been considered in this study, either because they came from impurities in benzene or because they were very small (hydroquinone). Phenol, nitrobenzene, and catechol came from benzene oxidation or nitration through reactions with reactive species containing oxygen and/or nitrogen (ROS and RNS, respectively) formed from the interaction plasma-air and/or plasma-liquid. Berndt and Bogë[46] have identified phenol and nitrobenzene as products resulting in gas-phase reactions of ·OH radicals with benzene in mixtures containing O_2 and NO.

Phenol is likely produced by oxidation of benzene through reactions with hydroxyl radicals ·OH:

$$C_6H_6 + \cdot OH \rightarrow C_6H_5OH \quad (7)$$

Subsequent oxidation of phenol to catechol might be achieved through further hydroxylation[47] (see **Figure 3**)

$$C_6H_5OH + \cdot OH \rightarrow C_6H_4(OH)_2 \quad (8)$$

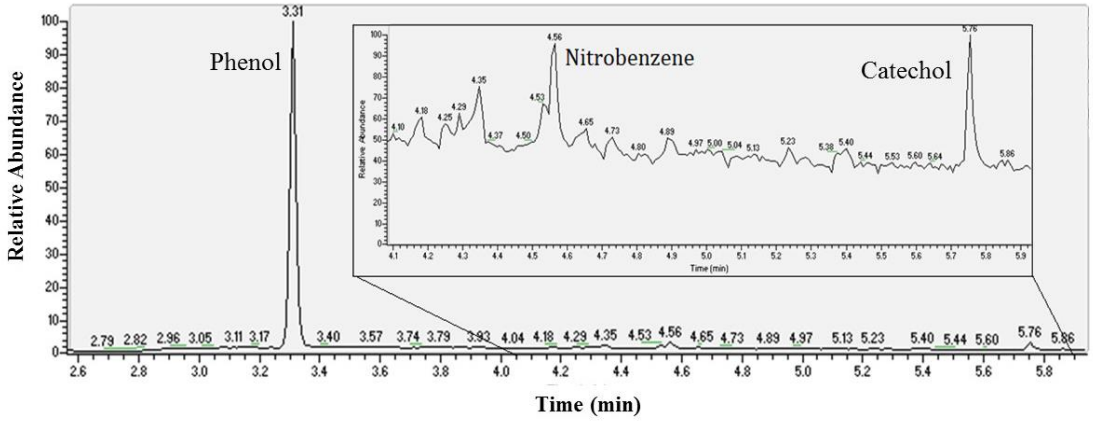

Figure 2. Chromatogram measured for P = 50 W, F = 1.5 L/min, d = 2 cm and t = 1 min.

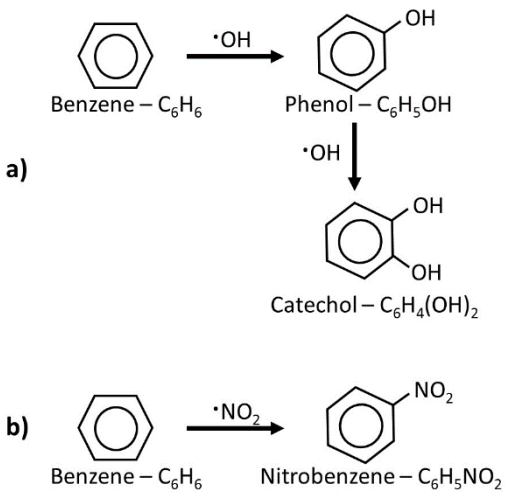

Figure 3. Oxidation and nitration products from plasma-benzene interaction

Nitrobenzene results from nitration of benzene by ·NO_2 long-lived species generated in the gas-liquid interface (see **Figure 3**).[47,48]

$$C_6H_6 + \cdot NO_2 \rightarrow C_6H_5NO_2 \quad (9)$$

In this work, a detailed study of the degradation of benzene under different experimental conditions was performed. In each case, the concentration of phenol, nitrobenzene, and catechol was measured. Next, the main results of this study are presented.

Figure 4a shows changes in phenol, nitrobenzene and catechol content of the treated samples under different microwave power conditions (30, 40, 50 and 60 W). In all cases, a growing dependence on power for the concentration of these products was found.

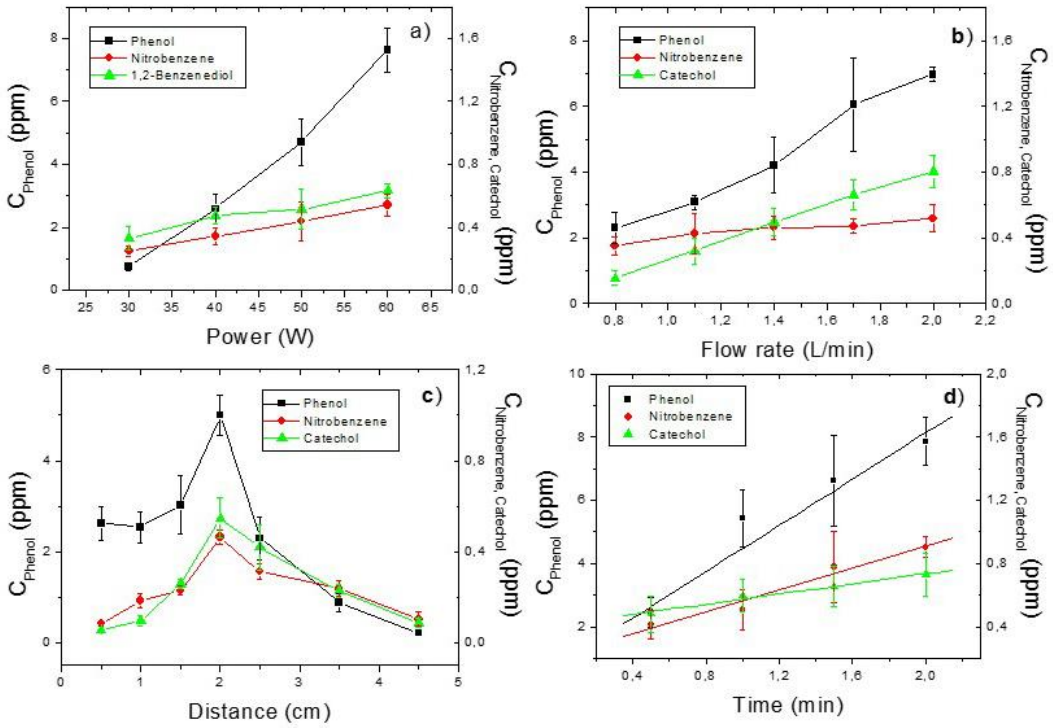

Figure 4. Dependence of phenol, nitrobenzene and catechol GC-MS concentrations on: a) power (F = 1.5 L/min, t = 1 min, d = 2 cm); b) gas flow rate (P = 50 W, t = 1 min, d = 2 cm); c) plasma-sample distance (P = 50 W, F = 1.5 L/min, t = 1 min); and d) treatment time (P = 50 W, F = 1.5 L/min, d = 2 cm).

Phenol was by far the main product resulting from the plasma action on the liquid sample, under these experimental conditions. Considering that the solubility of catechol in benzene is higher than in water, these results indicate that single hydroxylation of benzene was favored. The formation of catechol from benzene involves two steps, the first one producing phenol, whose concentration must increase in the reaction medium to yield an appreciable amount of catechol. These differences in the concentration of phenol and catechol produced during benzene degradation are also observed in bioremediation processes.[49] Interestingly, catechol and nitrobenzene behavior with power followed the same trend.

In order to understand the role played by argon excited species in the degradation process, the evolution with the power of the relative population of argon excited species *4p* in the region of the plasma closest to the liquid sample was studied (see **Figure 5a**).

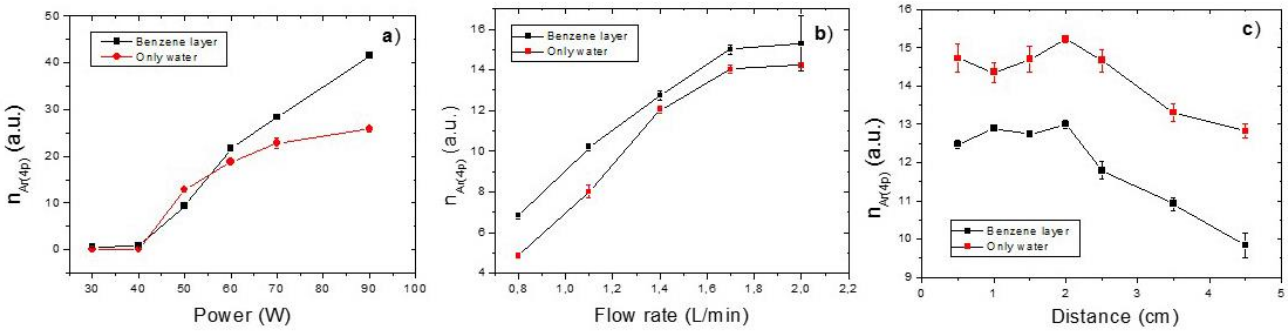

Figure 5. Dependence of the relative population of argon excited species *4p* in the cases of water with and without a benzene layer on: a) power (F = 1.5 L/min, t = 1 min, d = 2 cm); b) gas flow rate (P = 50 W, t = 1 min, d = 2 cm); c) plasma-sample distance (P = 50 W, F = 1.5 L/min, t = 1 min); and d) treatment time (P = 50 W, F = 1.5 L/min, d = 2 cm).

Unless for very low power conditions where intensity of emission lines was below the detection limit of the optical set-up and the density of argon excited species could not be measured, it was found that the amount of these species delivered by the plasma jet notably increases with the power, in the same way that concentrations of phenol and catechol do (see **Figure 4a**), evidencing the outstanding role of these species in ·OH formation. Argon excited species (energy ≥ 11.5 eV) striking on water molecules of the humid air at the gas phase between plasma and liquid are most likely leading to water dissociation in hydroxyl and hydrogen radicals (H-OH bond energy 5.2 eV)[50]

$$Ar^{*,m} + H_2O \rightarrow Ar + \cdot OH + \cdot H \qquad (10)$$

Also, in this plasma jet, excitation transfer reactions from argon metastables (Ar^m) to ground state of molecular nitrogen are the main mechanism to excite nitrogen molecules[21]

$$Ar^m + N_2 \rightarrow Ar + N_2^* \qquad \text{Energy threshold (11.5 eV)} \quad (11)$$

and these species might cause further dissociation of water molecules (although to a lesser extent because of the higher energy cost) through reactions[51]

$$N_2^* + H_2O \rightarrow N_2 + \cdot OH^* + \cdot H \quad (12)$$

On the other hand, the generation of reactive nitrogen species in plasma jets generally initiates with the formation of ·NO from N* reacting with O_2, and eventually, further reactions with other ROS and RNS result in the generation of species N_xO_y.[52] The following reactions have been proposed by Jablonowski et al. for ·NO formation in an argon plasma jet open to the air in:[50,53]

$$N_2^* + \cdot O \rightarrow \cdot NO + N \quad (13)$$

$$N + \cdot OH \rightarrow \cdot NO + \cdot H \quad (14)$$

Subsequent oxidation of ·NO by oxidizing agents such as O_3 or ·O leads to ·NO_2 formation[50,53]

$$\cdot NO + O_3 \text{ or } \cdot O \rightarrow \cdot NO_2 + \text{products} \quad (15)$$

Atomic oxygen in reactions (13) and (15) and nitrogen in (14) are likely generated from[7,50]

$$Ar^* + O_2 \rightarrow Ar + 2\ O \quad (16)$$

$$Ar^* + N_2 \rightarrow Ar + 2\ N \quad (17)$$

In short, the higher the power the greater the production of argon excited atoms, which is ultimately favoring reactions (10)-(17) leading to the formation of ·OH and ·NO_2 species responsible for benzene oxidation/nitration. The relatively high energy cost for N_2 excitation/dissociation (> 11.3 eV) triggering reactions (12)-(15) could explain the reduced formation of nitrobenzene, compared to phenol generation.

Figure 4b depicts the influence of the gas flow rate conditions on benzene degradation. For this purpose, concentrations of phenol, nitrobenzene, and catechol in samples were measured upon treatments with the jet working at 0.8, 1.1, 1.4, 1.7 and 2 L/min argon flow rates. In this case,

time of treatment, microwave power, and plasma-liquid distance were kept constant (P = 50 W, t = 1 min, d = 2 cm). Again, an increasing (approx. linear) relationship between the concentration of products and gas flow rate was found, in the range of flow rates studied. Remarkably, the concentration of nitrobenzene in samples showed a lesser dependence on gas flow-rate than phenol and catechol, whose production notably grew with this physical parameter. This is due to the fact that production of nitrobenzene is a two steps process, where in first instance, N_2 molecules are excited from collisons with argon excited species from plasma (Eq. 11) and, later, they eventually trigger reactions (12)-(15) leading to formation of NO_2.

Figure 5b shows the density of argon atomic excited species in states *4p* in the plasma region at the end of the column and its dependency on the argon flow rate. This figure also includes measurements performed when the liquid sample was just water (without the benzene layer on its top). The higher the flow rate, the higher the speed of the impinging gas jet, which pushed down the liquid surface. This dimpling caused recirculation in the liquid.[1,54] Thus, progressively higher flow rates led to deeper dimples (and to a better recirculation effect), which made the bulk of water underneath progressively more accessible, thus enhancing water releasing and evaporation (see **Figure 6**). Moreover, high flow rate conditions also favored the generation of argon excited species (see **Figure 5b**). The combination of these effects most likely increased the formation of ·OH radicals (only requiring energies of 5.2 eV) in both the gas and the liquid phase, which eventually resulted in more oxidation reactions, and higher concentrations of phenol and catechol. Conversely, nitration and so nitrobenzene formation was almost unaffected by changes of flow rate as, in this case, the amount of air in the plasma should not change significantly, and energies required for N_2 excitation triggering reactions (13)-(15) are considerably higher (> 11.3 eV).

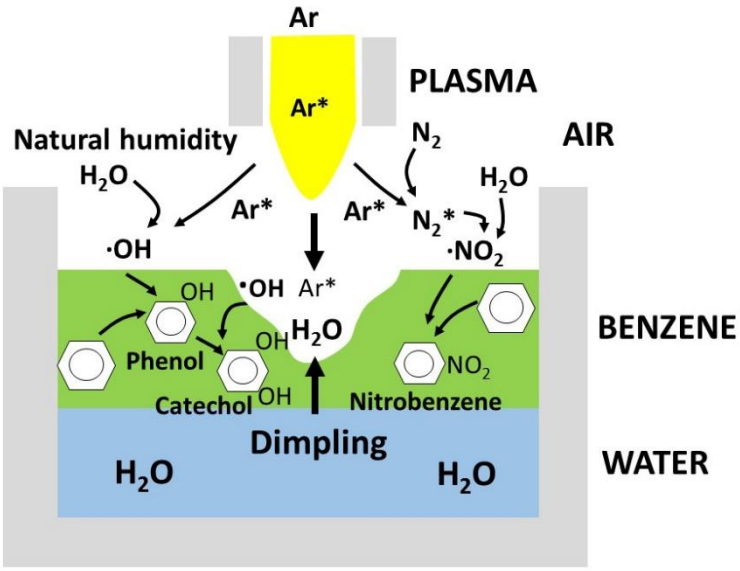

Figure 6. Plasma action on the benzene layer sample.

The influence of the plasma-sample distance on the benzene degradation was also explored. **Figure 4c** shows changes in phenol, nitrobenzene and catechol contents of the samples treated with the plasma jet (P = 50 W, F = 1.5 L/min, t = 1 min) placed at seven different distances from them. In all cases, a maximum was measured around 2 cm. Interestingly, the same dependency on the distance has been found for the relative density of argon atomic excited species *4p* in the plasma (see **Figure 5c**), which again evidences these species are likely playing an outstanding role in the process. Results in **Figure 5c** show that the presence of the liquid is affecting the plasma itself. At shorter distances, higher amounts of benzene at the gas phase most likely prevented the contact of air with the plasma, and so the quenching of argon excitation through reactions (11) that took place at longer distances.

Finally, **Figure 4d** shows results corresponding to changes in treatment times. In this case, plasma-sample distance (2 cm), microwave power (50 W) and gas flow rate (1.5 L/min) stayed fixed. Phenol was again by far the main product resulting from the plasma action. An increasing trend was found for phenol generation, and rather linear tendencies were detected for catechol

and nitrobenzene. In all cases, higher treatment times favored the degradation of benzene. From the linear fittings of these values, formation rates of 3.48, 0.16 and 0.35 ppm/min were measured for phenol, catechol, and nitrobenzene respectively (for the experimental conditions in **Figure 4d**).

3.2. Interaction plasma-water

For a better understanding of the benzene oxidation process induced by this plasma jet, its interaction with a water surface was also investigated. For this purpose, the amount of OH radicals generated in the sample of water upon plasma treatment was measured following the method proposed by Newton and Milligan[37] and used by Ceriani et al.[35] In this way, aqueous solutions of CCA were treated and the formation of CCA-7-OH was studied.

Typical fluorescence spectra measured for treated samples are shown in **Figure 7**. The height of peaks was measured by subtracting the intensity of the line at 400 nm to the intensity at 443 nm, which is the maximum of the peak. Three different measurements were made for each condition, although in **Figure 7** only averaged values are represented.

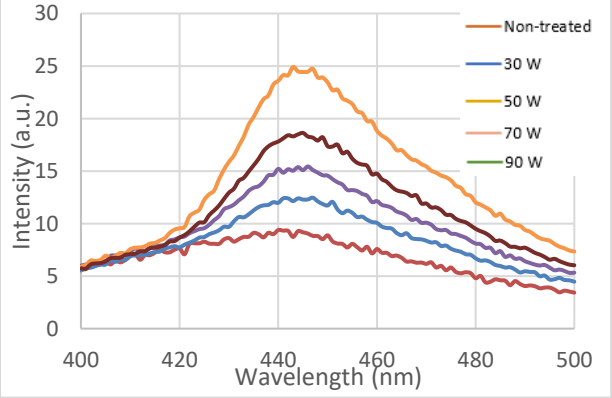

Figure 7. Fluorescence spectra for different microwave power

Changes in the concentration of CCA-7-OH under different experimental conditions (microwave power, argon flow rate, plasma-liquid distance, treatment time) were analyzed.

In the first instance, the dependency on the microwave power injected into the plasma was studied (see **Figure 8a**). For this purpose, microwave power was set from 30 to 90 W, while treatment time, gas flow rate and plasma-sample distance were kept constant.

As expected, an increasing relationship was found between CCA-7-OH concentration and microwave power (production rate of 0.02 ppm/W). Higher microwave powers lead to a greater ·OH production through reactions (10)-(12), because of both the higher amount of argon excited species (**Figure 5a**) and the greater evaporation of water. Indeed, **Figure 9a** shows the changes in the plasma gas temperature (at its end position, closer to the liquid) with power, so as expected, an increase of microwave power resulted in a raise of the gas temperature in the plasma, favoring evaporation.

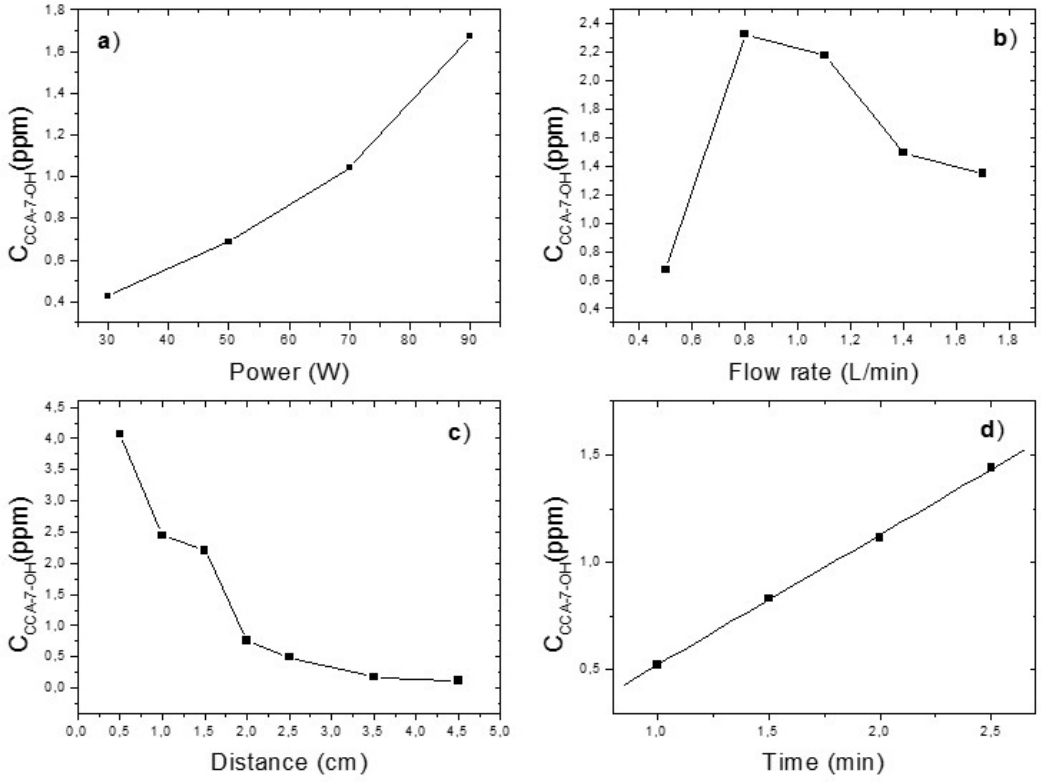

Figure 8. Dependence of the concentration of CCA-7-OH on: a) power (F = 1.5 L/min, t = 1 min, d = 2 cm); b) gas flow rate (P = 50 W, t = 1 min, d = 2 cm); c) plasma-sample distance (P = 50 W, F = 1.5 L/min, t = 1 min); and d) treatment time (P = 50 W, F = 1.5 L/min, d = 2 cm).

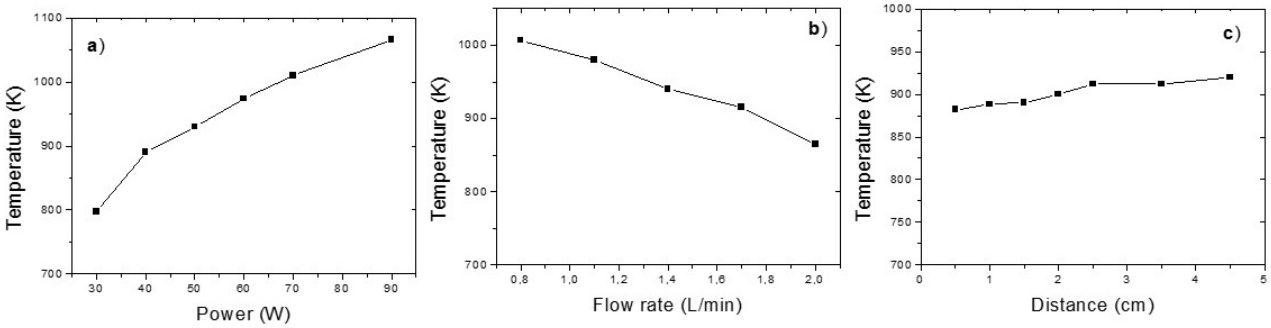

Figure 9. Variations of gas temperature in the plasma with: a) power (F = 1.5 L/min, t = 1 min, d = 2 cm); b) gas flow rate (P = 50 W, t = 1 min, d = 2 cm); and, plasma-sample distance (P = 50 W, F = 1.5 L/min, t = 1 min)

The influence of the gas flow rate on ·OH radical formation in water is shown in **Figure 8b** for P = 50 W, t = 1 min and d = 2 cm. Interestingly, unlike the growing tendency shown in **Figure 4b**, a maximum of OH formation was detected around 1 L/min. This different dependence on

the gas flow rate for benzene hydroxylation (resulting in phenol formation) and ·OH generation in CCA aqueous solutions, could be tentativelly ascribed to the dissimilar forms of plasma-liquid interaction taking place in each case. In the first case, because of its lower density, benzene forms a layer on the water surface precluding direct contact of the plasma species with water under it, so most reactions are likely taking place at the gas phase. As already mentioned, high gas flow rates lead to both higher amounts of argon excited species and a more effective liquid surface dimpling (favoring water evaporation), so resulting in a better interaction of the plasma species with water leading to ·OH formation.

In the second case, CCA is soluble in water and there is no physical barrier hampering water evaporation, so plasma species reach water easily. In this case, ·OH from evaporated water becomes more significant (see **Figure 10**). Moreover, chemistry in the bulk of the liquid (including oxidation of CCA) could be also relevant.[47,52,53]

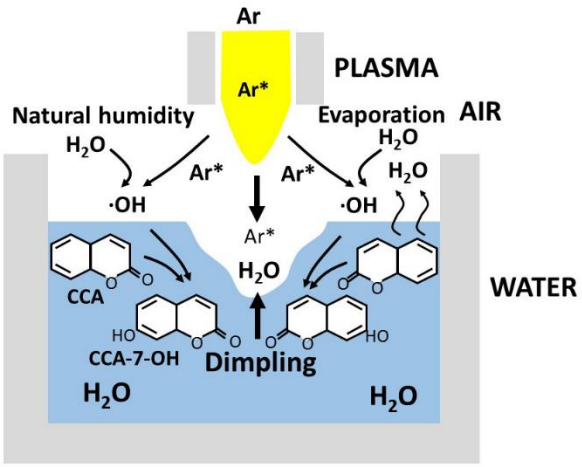

Figure 10. Plasma action on the aqueous solution sample

As shown in **Figure 8b**, an initial growing tendency with the gas flow rate is observed, but relatively high flow rates disfavor CCA oxidation to CCA-7-OH. In the beginning, a higher flow implies both faster evaporation and a greater amount of argon excited species generating ·OH radicals most likely at the gas phase. Figure 9b shows variations of the gas temperature at

the end part of the plasma with the argon flow rate. Plasma cooled down but the speed of the gas impinging the sample increased, so evaporation could be important. From a certain value of flow rate, CCA oxidation to CCA-7-OH did not grow anymore and for higher values, it even reduced. This fact could be tentatively explained considering the temperature of the plasma became 100 K smaller and most probably evaporation reduced. Moreover, under turbulent flow regime, interactions of the plasma jet with the liquid surface result in stronger disruption of the surface and ultimately, in a gas-liquid turbulent mixing [1] most probably favoring reactions leading to ·OH reduction:[47,52,53]

$$\cdot OH_{aq} + \cdot OH_{aq} \rightarrow H_2O_{2aq} \quad (18)$$

$$\cdot OH_{aq} + \cdot NO_{2aq} \rightarrow ONOOH_{aq} \rightarrow HNO_{3aq} \rightarrow H^+_{aq} + NO_3^-{}_{aq} \quad (19)$$

where subscript "aq" denotes species in the aqueous medium.

Results corresponding to changes in plasma-water distance are shown in Figure 8c. An exponential decrease was found. Again it can be seen that mechanisms ruling CCA oxidation are not fully controlled by argon excited species kinetics in this case (although ·OH radicals likely form from them). The highest CCA-OH-7 formation takes place at the shortest distance, case in which evaporation should be most important. At progressively longer distances, the amount of water vapor formed by the action of plasma diminishes (because the temperature near the liquid surface progressively reduces), and so the formation of ·OH does. **Figure 9c** shows small variations of the gas temperature in plasma when changing plasma-water distance.

Finally, **Figure 8d** depicts changes in CCA-7-OH concentration of the sample after different treatment times, for plasma-sample distance, microwave power and gas flow rate fixed. As in benzene experiments, the generation of CCA-7-OH has a linear dependency on the treatment time. A CCA oxidation rate of 0.61 ppm/min was found for the specific conditions P = 50 W, F = 1.5 L/min, d = 2 cm.

Making a rough estimate, in the 4 ml of a 0.003 M CCA solution, there were $7.28 \cdot 10^{18}$ molecules of CCA. Under the most favorable experimental conditions, plasma treatment led to the formation of $4.44 \cdot 10^{16}$ molecules of CCA-7, which implies that a total of $9.44 \cdot 10^{17}$ ·OH radicals (considering a 4.7% yield after Newton et al. method[37]) were generated through the plasma jet action. On the other hand, 1.5 ml of benzene contain $1.01 \cdot 10^{22}$ molecules resulting in $6.7 \cdot 10^{16}$ (8 ppm) phenol molecules, $5.0 \cdot 10^{15}$ (0.7 ppm) catechol molecules and $3.9 \cdot 10^{15}$ (0.6 ppm) nitrobenzene molecules. Thus, a total of $7.7 \cdot 10^{16}$ OH were approximately brought into play in oxidation reactions of benzene.

Finally, in these experiments, the electron density was also measured and for the three parameters studied (microwave power, flow rate and distance to the sample) an approximately constant value of n_e was obtained ($\sim 1.98 \times 10^{20}$ m^{-3}).

4 Conclusions

In this work, the interaction of an argon non-thermal microwave plasma jet with liquid was studied from the analysis of benzene degradation. Different operational conditions were investigated, including microwave power, argon flow rate, plasma-sample distance and time of treatment.

The main products formed from plasma action were phenol, catechol, and nitrobenzene, evidencing the formation of ·OH and $\cdot NO_2$ radicals at the gas phase. Since the treatment times of samples were always relatively short, only partial degradation of benzene was achieved.

Under the experimental conditions explored, phenol was by far the main product formed indicating that a single oxidation route was favored over double one. High treatment times favor the formation of phenol, catechol, and nitrobenzene, and ultimately, benzene degradation. On the other hand, changes in generation of phenol, catechol and nitrobenzene with microwave power, argon flow rate and plasma-sample distance followed the same trend as the population

of argon atomic excited species in states *4p* in the plasma did, which evidences the outstanding role of these species in the degradation process and reactions at the gas phase. Indeed, these species (with energies over 11.3 eV) seem to be most likely responsible for ·OH and $\cdot NO_2$ formation. Tentatively, the set of reactions (3)-(10) have been proposed as the routes ruling the generation of these radicals.

In order to clarify the origin of ·OH radicals oxidizing benzene, CCA-aqueous solutions were also treated, and using the method proposed by Newton et al. the amount of ·OH species formed in them were measured. A different form of plasma-liquid interaction was found in this case, mainly controlled by water evaporation.

Values of gas temperature in the plasma (ranging between 800 and 1100 K) evidences the cooling effect of the liquid sample on the plasma.

Finally, the electron density of the plasma jet was also measured and an approximately constant value of n_e was obtained ($\sim 1.98 \times 10^{20}$ m^{-3}), for the three parameters studied (microwave power, flow rate and distance to the sample).

Acknowledgements: The authors thank the European Regional Development Funds program (EU-FEDER) and the MINECO (project MAT2016-79866-R) for financial support. The authors also are grateful to the Polish National Agency for Academic Exchange as part of the Academic International Partnerships (project PPI/APM/2018/1/00033/U/001).

Received: ((will be filled in by the editorial staff)); Revised: ((will be filled in by the editorial staff)); Published online: ((please add journal code and manuscript number, e.g., DOI: 10.1002/ppap.201100001))

REFERENCES

[1] P.J. Bruggeman, M.J. Kushner, B.R. Locke, J.G.E. Gardeniers, W.G. Graham, D.B. Graves, R.C.H.M. Hofman-Caris, D. Maric, J.P. Reid, E. Ceriani, D. Fernandez Rivas, J.E. Foster, S.C. Garrick, Y. Gorbanev, S. Hamaguchi, F. Iza, H. Jablonowski, E. Klimova, J. Kolb, F. Krcma, P. Lukes, Z. Machala, I. Marinov, D. Mariotti, S. Mededovic Thagard, D. Minakata, E.C. Neyts, J. Pawlat, Z. Lj. Petrovic, R. Pflieger, S. Reuter, D.C. Schram, S. Schröter, M, Shiraiwa, B. Tarabová, P.A. Tsai, J.R.R Verlet, T. von Woedtke, K.R. Wilson, K. Yasui, G. Zvereva, *Plasma Sources Sci. Technol.* **2016**, *25*, 053002.

[2] F. Rezaeiet, P. Vanraes, A. Nikiforov, R. Morent, N. De Geyter, *Materials* **2019**, *12*, 2751.

[3] G. Daeschlein, S. Scholz, R. Ahmed, A. Majumdar, T. von Woedtke, H. Haase, M. Niggemeier, E. Kindel, R. Brandenburg, K. D. Weltmann, M. Jünger, *Journal of the German Society of Dermatology*, **2012**, *10*, 509.

[4] M. Ishaq, K.Bazaka, K.Ostrikov, *J. Phys. D: Appl. Phys.*, **2015**, *48*, 464002.

[5] M.C. Jacofsky, C.L. Lubahn, C. McDonnell, Y. Seepersad, G. Fridman, A. Fridman, D. Dobrynin, *Plasma Medicine*, **2014**, *4*, 177.

[6] S. Hasse, *Plasma Medicine*, **2014**, *4*,117.

[7] S. Reuter, T. von Woedtke, K.D. Weltmann, *J. Phys. D: Appl. Phys.*, **2018**, *51*, 233001.

[8] A. Khlyustova, C. Labay, Z. Machala, M.P. Ginebra, C. Canal, Front. Chem. Sci. Eng., **2019**, 13, 238.

[9] K. Song, G. Li, Y. Ma, *Plasma Medicine*, **2014**, *4*, 193.

[10] T. Woedtke, S. Reuter, K. Masur, K.D. Weltmann, *Physics Reports*, **2013**, *530*, 291.

[11] K. Zhigagn, P. Thopan, G. Fridman, V. Miller, L.D. Yu, A. Fridman, Q. Huang, *Clinical Plasma Medicine*, **2017**, *7–8*, 1.

[12] M. Laroussi, X. Lu, *Appl. Phys. Lett.*, **2005**, *87* 113902.

[13] M. Laroussi, C. Tendero, X. Lu, S. Alla, W.L. Hynes, *Plasma Process. Polym.*, **2006**, *3* 470.

[14] M. Laroussi, *IEEE Trans. Plasma Sci*., **2009**, *37*, 714.

[15] D.B. Graves, *J. Phys. D: Appl. Phys.*, **2012**, *45*, 263001.

[16] J.E. Foster, *Physics of Plasmas*, **2017**, *24*, 055501.

[17] B. Jiang, *Chem. Eng. J.*, **2014**, *236*, 348.

[18] P. Vanraes, A.Y. Nikiforov, C. Leys (**2016**). Electrical Discharge in Water Treatment Technology for Micropollutant Decomposition, Plasma Science and Technology - Progress in Physical States and Chemical Reactions, Tetsu Mieno, IntechOpen, DOI: 10.5772/61830. (Available from: https://www.intechopen.com/books/plasma-science-and-technology-progress-in-physical-states-and-chemical-reactions/electrical-discharge-in-water-treatment-technology-for-micropollutant-decomposition, (accessed February, 2020).

[19] P. Lukes, M. Clupek, V. Babicky, V. Janda, P. Sunka, *J. Phys. D. Appl. Phys.*, **2005**, *38*, 409.

[20] J. Foster, B. S.Sommers, S.N. Gucker, I.M. Blankson, G. Adamovsky, *IEEE Trans. Plasm. Sci.*, **2012**, *40*, 1311.

[21] M. C. García, M. Mora, D. Esquivel, J.E. Foster, A. Rodero, C. Jimenez-Sanchidrián, F.J. Romero-salguero, *Chemosphere*, **2017**, *180*, 239.

[22] Agency for Toxic Substances and Disease Registry (**2007**), (https://www.atsdr.cdc.gov/toxguides/toxguide-3.pdf) (accessed February, 2020).

[23] I. Kornev, S. Preis, *J. Adv. Oxid. Technol*, **2016**, *19*, 28.

[24] E.K. Wilson, (**2018**), *California wildfires caused unexpected benzene contamination of drinking water*, Chemical and Engineering News 96 (26) (https://cen.acs.org/environment/water/California-wildfires-caused-unexpected-benzene/96/i26) (accessed February, 2020).

[25] B. Saha, Ph.D. Thesis (2011), University of Windsor, Electronic Theses and Dissertations 408, *Removal of benzene from wastewater by enzyme-catalyzed oxidative polymerization combined with a modified Fenton reaction*. (https://scholar.uwindsor.ca/etd/408) (accessed February, 2020).

[26] M. Mohajerani, M. Mehrvar, F. Ein-Mozaffari, *Int. J. Eng.*, **2009**, *3*, 120.

[27] A. Anpilov, E.M. Barkhudarov, Y. B. Bark, Y.V. Zadiraka, M. Christofi, Y.N Kozlov, I.A. Kossyi, V.A. Kop'ev, V.P. Silakov, M.I. Taktakishvili, S.M. Temchin, *J. Phys. D Appl. Phys.*, **2001**, *34*, 993.

[28] P. Lukes, B.R. Locke, *J. Phys. D Appl. Phys.*, **2005**, *38*, 4074.

[29] K. Sato, K.Yasuoka, *IEEE Trans. Plasma Sci.*, **2008**, 36, 1144.

[30] G.R Stratton, C.L. Bellona, F. Dai, T.M. Holsen, S.M. Thagard, *Chem. Eng. J.*, **2015**, *273*, 543.

[31] S. Manolache, V. Shamamian, F. Denes, *J. of Environ. Engin.*, **2004**, *130*, 17.

[32] X.T. Deng, J.J. Shi, M.G. Kong, *J. Appl. Phys.*, **2007**, *101*, 074701 .

[33] A. Hamdan, J.L. Liu, M.S. Cha, *Plasm. Chem. Plasm. Proc.*, **2018**, *38*, 1003.

[34] A. Bansode, S.E. More, E.A. Siddiqui, S. Satpute, A. Ahmad, S.V. Bhoraskar, V.L. Mathe, *Chemosphere*, **2017**, *167*, 396.

[35] E. Ceriani, E.Marotta, V.Shapoval, G. Favaro, C. Paradisi, *Chem. Eng. J.*, **2018**, *337*, 567.

[36] M. Moisan, J. Pelletier, in *Microwave excited plasmas*, Plasma Technology, Elsevier, Amsterdam, **1992**, Ch. 3.

[37] Q.S. Yu and H.K. Yasuda, Plasma Chemistry and Plasma Processing, **1998**, 18, 461-485.

[37] G.L. Newton, J.R. Milligan, *Radiat. Phys. Chem.*, **2006**, *75*, 473.

[38] F.J. Bosi, F. Tampieri, E. Marotta, R. Bertani, D. Pavain, C. Paradisi, *Plasma Process. Polym.*, **2018**, *15*, e1700130.

[39] M.C. Garcia, A. Rodero, A. Sola, A. Gamero, *Spectrochim. Acta B*, **2000**, 55, 1733.

[40] I. Santiago, M. Christova, M.C. García, M.D. Calzada, *Eur. Phys. J. Appl. Phys.*, **2004**, *28* 325.

[41] Q.S. Yu, H.K. Yasuda, Plasma Chem. Plasma Process., **1998**, *18*, 461.

[42] A. Rodero, M.C. García, *J. Quant. Spec. Rad. Transfer.*, **2017**, *198*, 93.

[43] C. Yubero, M.D. Calzada, M.C. García, *J. Phys. Soc. Jpn.*, **2005**, *74*, 2249.

[44] M.C. Garcia, S.N. Gucker, J.E Foster, *J. Phys. D: Appl. Phys.*, **2015**, *48*, 355203.

[45] A. Nikiforov, C. Leys, M.A. Gonzalez, J.L. Walsh, *Plasma Sources Sci. Technol.*, **2015**, *24*, 034001.

[46] T. Berndt, O. Böge, *Phys. Chem. Chem. Phys.*, **2001**, *3*, 4946.

[47] P. Lukes, E. Dolezalova, I. Sisrova, M. Clupek, *Plasma Sources Sci. Technol.*, **2014**, 23, 015019.

[48] V.I. Parvulescu, M. Magureanu, P. Lukes, in Plasma Chemistry and Catalysis in Gases and Liquids, Wiley, **2012**, Ch. 7.

[49] Y. Tao, A. Fishman, W.E. Bentley, T.K. Wood, *Appl. Environ. Microbiol.*, **2004**, *70*, 3814.

[50] A. Schmidt-Bleker, J. Winter, A. Bösel, S. Reuter and KD Weltmann, *Plasma Sources Sci. Technol.*, **2016**, *25*, 015005.

[51] M. Magureanu, D. Piroi, F. Gherendi, N.B. Mandache, V. Parvulescu, *Plasma Chem. Plasma Process.*, **2008**, *28*, 677e688.

[52] A.M. Lietz and M.J. Kushner, *J. Phys. D: Appl. Phys.*, **2016**, *49*, 425204.

[53] H. Jablonowski, A. Schmidt-Bleker, K-D. Weltmann, T. von Woedtke, K. Wende, Phys. Chem. Chem. Phys., **2018**, *20*, 25387.

[54] J.F.M. van Rens, J.T. Schoof, F.C. Ummelen, D. C. van Vugt, P.J. Bruggeman, E.M. van Veldhuizen, *IEEE Trans. Plasma Sci.*, **2014**, *42*, 2622.

Graphical Abstract

This study looks into the formation of hydroxyl and nitrate radicals by an argon plasma jet through analysis of reactions between them and a sheet of benzene on water. CCA-aqueous solutions have been also treated and a different form of plasma-liquid interaction was found, mainly controlled by water evaporation.

Enrique Casado, Maria C. Garcia, Dorota A. Krawczyk, Francisco-José Romero-Salguero, Antonio Rodero[1]

Title Study of the plasma-liquid interaction for an argon non-thermal microwave plasma jet from the analysis of benzene degradation

ToC figure ((Please choose one size: 55 mm broad × 50 mm high **or** 110 mm broad × 20 mm high. Please do not use any other dimensions))